0013-7227/99/$03.00/0
Endocrinology

Vol. 140, No. 3
Printed in U.S.A.

Characterization of the Neuroanatomical Distribution of Agouti-Related Protein Immunoreactivity in the Rhesus Monkey and the Rat*

CARRIE HASKELL-LUEVANO†, PEILIN CHEN†, CHIEN LI*, KANG CHANG, M. SUSAN SMITH, JUDY L. CAMERON, AND ROGER D. CONE

Vollum Institute (C.H.-L., R.D.C.), Oregon Regional Primate Research Center (P.C., C.L., M.S.S., J.C.) Oregon Health Sciences University, Portland, Oregon 97201; and Phoenix Pharmaceuticals, Inc. (K.C.), Mountain View, California 94043

ABSTRACT

Agouti-related protein (AGRP) is a recently described homolog of the skin agouti protein. AGRP is transcribed primarily in the adrenal and hypothalamus and is a high affinity antagonist of the neural melanocortin-3 and melanocortin-4 receptors. The perikarya expressing AGRP messenger RNA are found in the arcuate nucleus of the rat and rhesus monkey. Using a polyclonal antibody against the pharmacologically active domain of AGRP (amino acids 83–132), we have also characterized the distribution of AGRP-immunoreactive neurons in both species. The major fiber tracts are conserved in both species, with dense projections originating in the arcuate nucleus and proceeding along the third ventricle. Dense fiber bundles are also visible in the paraventricular, dorsomedial, and posterior nuclei in the hypothalamus, in the bed nucleus of the stria terminalis, and in the lateral septal nucleus of the septal region. AGRP-containing neurons are not visualized in a number of areas, including portions of the amygdala, thalamus, and brain stem, that express MC3-R and MC4-R messenger RNA and receive innervation from POMC neurons that serve as the source of melanocortin agonists. Thus, AGRP is most likely to be involved in modulating a conserved subset of the physiological functions of central melanocortin peptides. Based on the particular distribution of AGRP neurons, those functions are likely to include the central control of energy homeostasis. (*Endocrinology* **140:** 1408–1415, 1999)

POMC, THE precursor of the melanocortin peptides (α-MSH, β-MSH, γ-MSH, and ACTH), is expressed in the brain exclusively in neuronal cell bodies throughout the rostrocaudal extent of the arcuate nucleus (ARC) and periarcuate area of the hypothalamus and within the caudal half of the commissural nucleus of the solitary tract (1–5). Proceeding from rostral to caudal, arcuate POMC cells send a dense bundle of fibers ventral to the anterior commissure, to a number of nuclei in the septal region, including the bed nucleus of the stria terminalis and lateral septal nucleus (LS), as well as to the nucleus accumbens in the caudate putamen. More caudally, fibers are seen projecting to the periventricular region of the thalamus and to the medial amygdala. Within the hypothalamus, the densest fibers project to the periventricular nucleus, the paraventricular nucleus (PVH), and the perifornical region, with some fibers seen in almost all hypothalamic regions. Finally, arcuate POMC fibers also project to several regions of the brain stem, including the periaquaductal gray, reticular formation, and parabrachial nucleus.

In situ binding studies using [^{125}I]Nle^{4},D-Phe^{7}-α-MSH have demonstrated that α-MSH binding sites correlate well with POMC terminal fields in the forebrain (6) and brain stem (7). Furthermore, the distribution of expression of the MC3-R and MC4-R in the rat central nervous system (CNS), determined by *in situ* hybridization (8–11), can easily account for the majority, if not all, of the melanocortin binding demonstrated in the CNS.

The central melanocortin system, as defined above by POMC neurons and the central MC3-R and MC4-R receptors, was recently given an added level of complexity by the discovery of agouti-related protein (AGRP) (12, 13). This 132-amino acid peptide is a homolog of the skin agouti peptide. The skin agouti peptide has previously been demonstrated to be an antagonist of the melanocortin-1 receptor (14) on melanocytes, where it is involved in the inhibition of eumelanin, or brown-black pigment, synthesis. The existence of a brain-specific agouti was suggested by the observation that the skin agouti peptide was also a high affinity antagonist of the neural MC4-R receptor (14) and caused an obesity syndrome when expressed ectopically in mouse strains containing certain dominant alleles of the gene (15–17). This obesity syndrome appears to result specifically from blockade of MC4-R signaling, as shown both pharmacologically and by gene knockout of the MC4-R (18, 19), suggesting that one function of POMC neurons involves the control of energy homeostasis.

In addition to being expressed in the arcuate nucleus, AGRP is also a potent antagonist of both the MC3-R and MC4-R (13, 20). As might be predicted, ubiquitous expression of a β-actin promoter/AGRP gene in transgenic mice (13, 21) results in an obesity syndrome comparable to that seen in mice with dominant agouti alleles such as A^{VY} (22) and in MC4-RKO mice (19). POMC neurons and the MC4-R

Received August 3, 1998.
Address all correspondence and requests for reprints to: Dr. Roger D. Cone, Vollum Institute L-474, Oregon Health Sciences University, 3181 SW Sam Jackson Park Road, Portland, Oregon 97201. E-mail: cone@ohsu.edu.
* This work was supported by NIH Grants DK-51730 (to R.D.C.), RR-00163 and HD-14643 (to M.S.S.), and HD-26888 (to J.L.C.).
† These authors contributed equally to this manuscript.

have been demonstrated to be involved in a number of processes other than energy homeostasis, however, including grooming behavior (23), control of fever (24), and cardiovascular homeostasis (25). Thus, determination of the potential physiological roles for AGRP requires characterization of the distribution of this protein in the CNS to identify MC3-R- and MC4-R-containing sites that may be coregulated by melanocortin agonists and the AGRP antagonist. Using a specific antibody to the C-terminal portion of this protein, we show here the distribution of AGRP immunoreactivity in the rat and rhesus monkey.

Materials and Methods

Animals

Rats. Female Sprague-Dawley rats (n = 8; B & K Universal, Inc., Kent, WA), weighing 240–260 μg, were housed in a room with a 12-h light, 12-h dark cycle (lights on at 0700 h) and constant temperature (23 $\pm$ 2 C). Food and water were provided *ad libitum*. Vaginal smears were examined daily to check the stage of the estrous cycle for each animal. Four animals were killed by decapitation during the diestrous stage of the cycle. Brains were removed, frozen on dry ice, and stored at -80 C until used for *in situ* hybridization. The remaining four animals were killed by perfusion as described below. All animal procedures involving rats were approved by the Oregon Regional Primate Research Center Institutional Animal Care and Use Committee.

Perfusion and tissue sectioning: Rats were anesthetized with a lethal dose of pentobarbital (125 mg/kg BW, ip) and perfused transcardially with 150 ml 2% sodium nitrite in saline followed by 150 ml 2.5% acrolein (EM grade, Polysciences, Warrington, PA) in phosphate-buffered 4% paraformaldehyde (pH 7.4). The brain was removed, blocked, and immersed in 25% sucrose at 4 C overnight. Coronal sections (25 μm) were cut through the whole brain on a sliding microtome and collected in a one in six series. The tissue sections were stored at -20 C in multiwell tissue culture plates containing cryoprotectant until use.

Rhesus monkeys. Hypothalamic and brain stem tissues from adult male rhesus monkeys (*Macaca mulatta*), weighing 8.9–10.2 kg, were used for this study. Monkeys were maintained in single animal cages in a room with a controlled lighting schedule (lights on, 0700–1900 h) and were fed one meal a day at approximately 1100 h of about 600 Cal high protein monkey chow (Ralston Purina Co., St. Louis, MO), with water available at all times. At least 1 month before death, monkeys had indwelling iv and intragastric catheters implanted using sterile surgical techniques, as previously described (26, 27). Catheters exited the body at the midscapular region of the back, and monkeys were maintained in jacket/tether/swivel systems (27), with the catheters running from the top of the swivel through a hole in the wall behind the monkey's cage to enter an adjacent room. Catheter patency was maintained by a constant saline infusion through the catheters of 100 ml/day, with the venous drip containing 400 U sodium heparin. Before death, all monkeys had been fasted at least one time and had received at least one meal via the gastric cannula, and blood samples had been collected and assayed for insulin and T_3 to ensure that the metabolic changes expected to occur with fasting and feeding were detectable. This study was approved by the

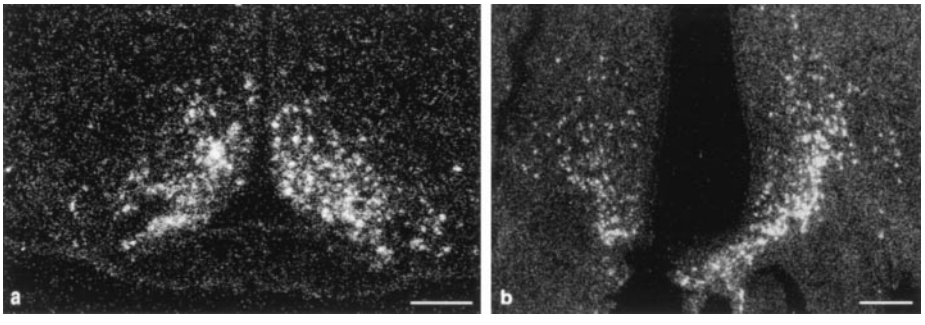

FIG. 1. *In situ* hybridization demonstrating that AGRP mRNA is expressed in the ARC of the rat (a) and the infundibular nucleus (In) of the rhesus monkey (b). A 400-bp human AGRP probe was transcribed in the presence of [^{33}P]UTP and hybridized to sections from the diestrous rat and fasted male rhesus monkey. *Bar*, 20 μm in a and 50 μm in b.

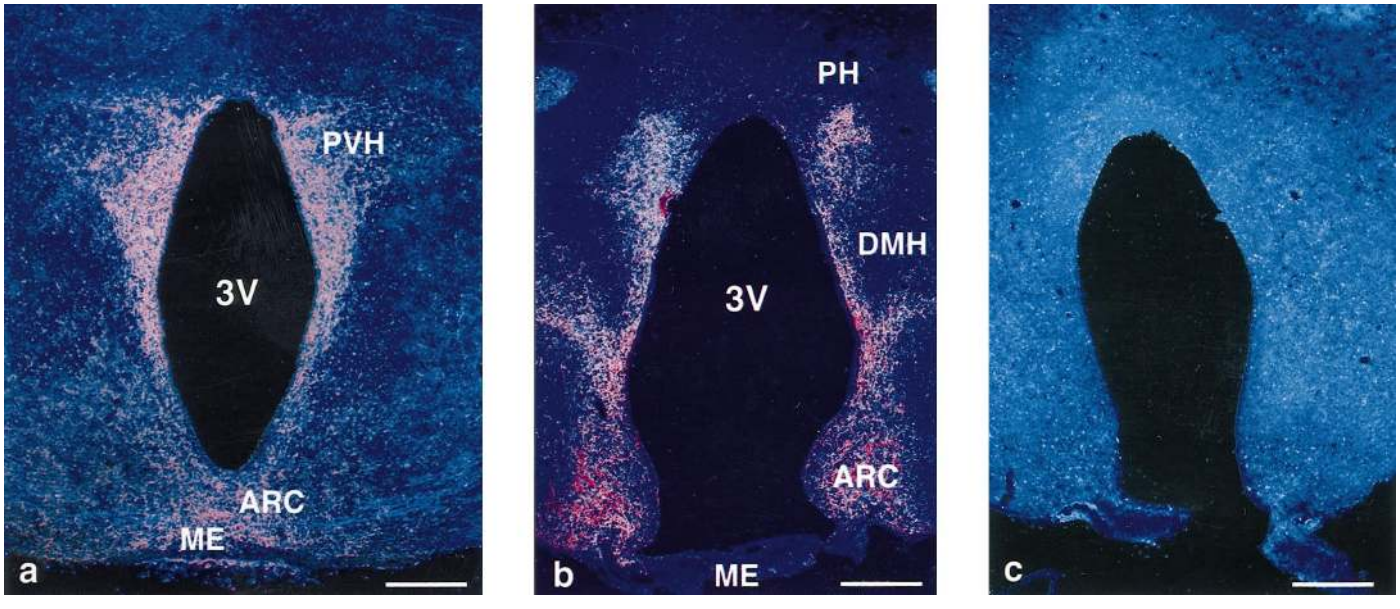

FIG. 2. Immunohistochemistry demonstrates dense hypothalamic neuronal fibers expressing AGRP in the diestrous rat. AGRP immunoreactivity is found in hypothalamic fibers projecting from the ARC as well as in the PVH (a) and DMH and PH nuclei (b). Preabsorption with the immunizing peptide AGRP-(83–132) blocks the staining reaction (c). *Bars*, 100 μm.

institutional animal care and use committee of the University of Pittsburgh.

Perfusion and tissue sectioning: Monkeys were fasted the day before death, and on the morning of death a fed monkey received an infusion of 200 ml nutrients (containing 600 Cal, with the same percentage of protein, carbohydrate, and fat as the standard monkey chow) (26) via the gastric cannula from 0630–0730 h, whereas the fasted animal did not. At 1025 h monkeys were sedated with ketamine HCl (10 mg/kg, im), and deeply anesthetized with sodium pentobarbital (~15 mg/kg, iv). The chest was then opened by a midline incision, and each monkey was perfused transcardially with 0.9% NaCl containing 2% sodium nitrite (800–1000 ml) to flush blood from the vascular system, followed by 4% paraformaldehyde in 0.1 M potassium phosphate buffer solution (KPBS; pH 6.8–7.2; 1000–1200 ml). The brain and upper portion of the spinal cord were removed, hypothalamic and brain stem tissue blocks were cut, and blocks were immersed in a postperfusion fixative of 2.5% acrolein and 4% paraformaldehyde-KPBS solution for 2 h at 25 C, followed by placement in a 25% sucrose solution in distilled water at 4 C for 4–6 days until they sunk to the bottom of the sucrose solution. Fresh sucrose solution was replaced daily. The hypothalamus was sectioned (30-μm sections) on a coronal plane using a freezing microtome, and sections were stored in cryoprotectant at −20 C until immunocytochemical and *in situ* hybridization procedures were performed. Due to the limited number of animals available for this study, the data presented here result from analysis of one fasted and one fed rhesus monkey.

Immunohistochemistry

Both monkey and rat sections were processed at the same time to ensure uniformity of immunostaining. Tissue sections were removed from cryoprotectant and rinsed in 0.05 M KPBS followed by treatment with 1% $NaBH_4$-KPBS solution (Sigma Chemical Co., St. Louis, MO). Sections were incubated in rabbit anti-AGRP antibody (G-003–53; 1:35,000; Phoenix Pharmaceuticals, Inc., Mountain View, CA) in KPBS with 0.4% Triton X-100 at 4 C for 48 h. Control sections were preabsorbed with 20 μg AGRP-(83–132) peptide to 1 μg antibody to test the specificity of the antibody. After rinsing in KPBS, the sections were incubated for 1 h at room temperature in biotinylated goat antirabbit IgG (1:600, Vector Laboratories, Inc., Burlingame, CA), followed by 10-min incubation in tyramide signal amplification solution according to the manufacturer's instruction (TSA-Indirect kit, New England Nuclear Life Science, Boston, MA). The antibody-peroxidase complex was stained with a mixture of 3,3′-diaminobenzidine and H_2O_2 in 0.05 M Tris buffer-saline solution. After the staining, tissue sections were mounted on gelatin-coated glass slides and air-dried. The 3,3′-diaminobenzidine staining on the tissue sections was further enhanced by osmium tetroxide (OsO_4), as described previously (28), before being coverslipped with Histomount (Fisher Scientific, Pittsburgh, PA).

In situ hybridization

Monkey brain. A 399-bp human AGRP complementary DNA was generated by PCR and subcloned into the pBSII SK(±) vector (Stratagene, La Jolla, CA). The human (h) AGRP complementary RNA (cRNA) probe was transcribed from the vector with 40% of the UTP provided in a ^{33}P-labeled form (New England Nuclear Life Science, Boston, MA) (29). The specific activity of the probe ranged from 1–2 × 10^9 dpm/μg. Brain sections were rinsed in PBS and treated with 1% $NaBH_4$-PBS solution. After washing with 0.25% acetic anhydride in 0.1 M triethanolamine (pH 8.0) and in 2 × SSC, sections were incubated in prehybridization solution containing 50% formamide, 6.25% dextran sulfate, 0.7% Ficoll, 0.7%

TABLE 1. Distribution of AGRP immunoreactivity in the rat central nervous system

Abbreviation	Anatomical brain region	Density
AHC	Anterior hypothalamic area, central part	+
ArcD	Arcuate n., dorsal part	+++
ArcL	Arcuate n., lateral part	+++
ArcM	Arcuate n., medial part	+++
ArcMP	Arcuate n., medial posterior part	+++
AVPe	Anteroventral periventricular n.	++
BSTL	Bed n. of stria terminalis, lateral division	+
BSTMA	Bed n. of stria terminalis, medial division, anterior part	++
BSTMPM	Bed n. of stria terminalis, medial division, posteromedial part	++
BSTMV	Bed n. of stria terminalis, medial division, ventral part	++
DMHd	Dorsomedial hypothalamic n., dorsal part	++
DMHv	Dorsomedial hypothalamic n., ventral part	++
DTM	Dorsal tuberomammillary n.	++
LH	Lateral hypothalamic n.	+
LSV	Lateral septal n., ventral part	++
ME	Median eminence	+
MM	Medial mammillary n., medial part	+
MMn	Medial mammillary n., median part	+
MPO	Medial preoptic n.	+
MPOL	Medial preoptic n., lateral part	+
PaAP	Paraventricular hypothalamic n., anterior parvicellular part	++
PaPo	Paraventricular hypothalamic n., posterior part	++
PaV	Paraventricular hypothalamic n., ventral part	++
PaAP	Paraventricular hypothalamic n., anterior parvicellular part	+
PaMP	Paraventricular hypothalamic n., medial parvicellular part	++
PaDC	Paraventricular hypothalamic n., dorsal cap	+
PH	Posterior hypothalamic area	++
Pe	Periventricular n.	++
PS	Parastrial n.	+
PVP	Paraventricular thalamic n., posterior part	+
RCh	Retrochiasmatic area	++
VDB	N. of the vertical imb of the diagonal band	+
VMHDM	Dorsomedial part of the ventromedial n.	+
VMPO	Ventral preoptic n., anterior	+
ZI	Zona incerta	++

Semiquantitative estimates of the signals are indicated based upon the number of fibers observed within a given area: + (weak); ++ (moderate); +++ (strong). Nomenclature is defined according to (37).

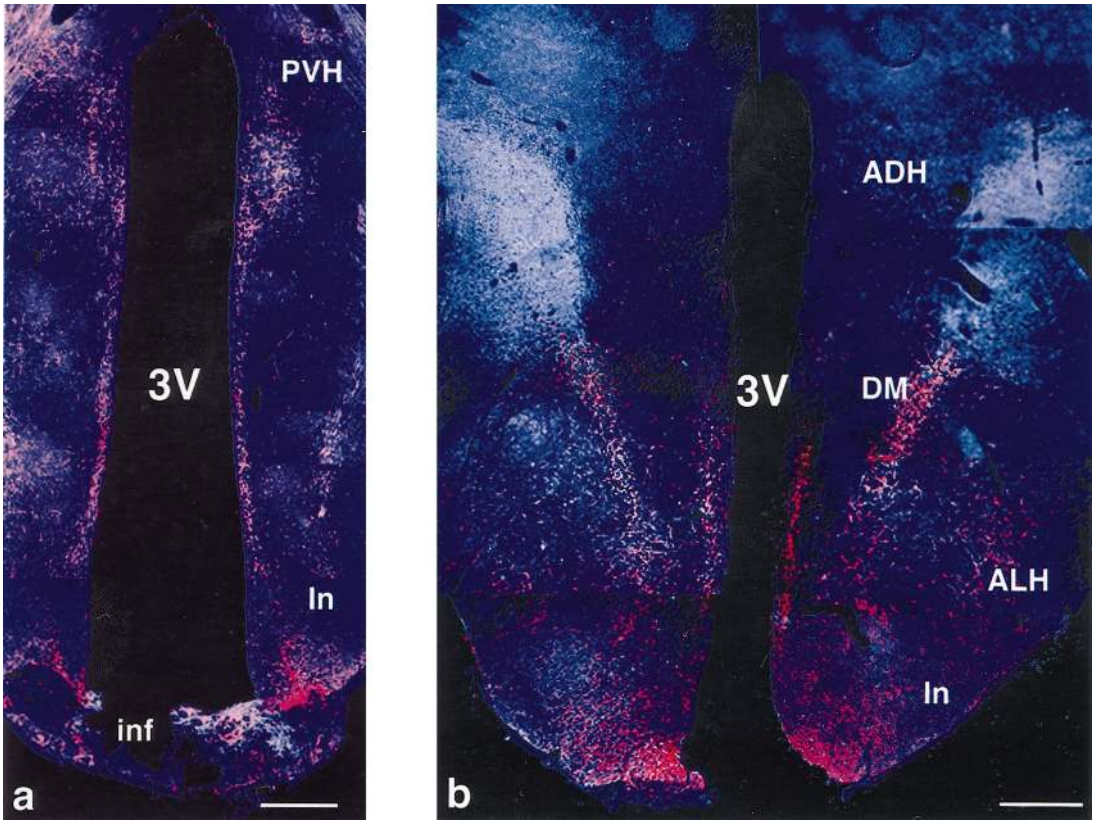

FIG. 3. Immunohistochemistry demonstrates dense hypothalamic neuronal fibers expressing AGRP in a fasted male rhesus monkey. AGRP immunoreactivity is found in hypothalamic fibers projecting from the infundibular nucleus (In) as well as in the PVH (a) and DMH nuclei (b). *Bars*, 100 μm.

polyvinyl pyrolidone, and 2 mg/ml yeast transfer RNA for 2 h at 55 C. Subsequently, sections were incubated in the same solution, with the addition of 1.5×10^5 cpm/μl antisense (or sense) cRNA probe for 15 h at 55 C. After hybridization, sections were washed in 4 × SSC (standard saline citrate), digested with ribonuclease A for 30 min at 37 C, and washed through decreasing concentrations of SSC to a final stringency of 0.1 × SSC at 60 C for 30 min. Sections were mounted on gelatin-coated glass slides and allowed to dry. The slides were dipped in NTB-2 emulsion (Eastman Kodak Co., Rochester, NY), exposed for 7–8 days at 4 C, and developed. After development, the slides were dehydrated, counterstained with cresyl violet, and coverslipped in Histomount.

Rat brain. Human AGRP cRNA probe was synthesized and used for *in situ* hybridization as described above. Briefly, the hAGRP cRNA probe was transcribed from a 399-bp complementary DNA in which 40% of the UTP was ^{35}S labeled (New England Nuclear Life Science, Boston, MA). The saturating concentration of the probe used in the assay was 1.0 μg/ml. The specific activity of the probe ranged from $8–9 \times 10^8$ dpm/μg. *In situ* hybridization was performed as described previously (29). Frozen brain sections (20 μM) were fixed in 4% paraformaldehyde and treated with a fresh solution containing 0.25% acetic anhydride in 0.1 M triethanolamine (pH 8.0), followed by a rinse in 2 × SSC, dehydrated through a graded series of alcohols, delipidated in chloroform, rehydrated through a second series of alcohols, and then air-dried. The slides were exposed to the hAGRP cRNA probe overnight in moist chambers at 55 C. After incubation, the slides were washed in ribonuclease-containing SSC that increased in stringency up to a wash in 0.1 × SSC at 60 C, then dehydrated through a graded series of alcohols and air-dried. Slides were dipped in NTB-2 emulsion (Eastman Kodak Co., Rochester, NY), exposed for 7–8 days at 4 C, and developed. After development, the slides were coverslipped with Histomount.

Results

Expression of AGRP messenger RNA (mRNA) in the rat and rhesus brain

Using *in situ* hybridization, AGRP-positive signals in the rat were observed predominantly in the ARC (Fig. 1a). AGRP-positive signals in the rhesus were detected in the comparable structure in the primate, known as the infundibular nucleus, in the fasted animal (Fig. 1b). No signal was detected in tissue from the fed animal (not shown).

AGRP immunoreactivity in the Rat CNS

The studies described below were performed with a polyclonal antibody against a biologically active C-terminal fragment (amino acids 83–132) of the human AGRP prepared using synthetic methods (30). AGRP gene expression has been demonstrated to be elevated in the *ob/ob* mouse (12), and high levels of AGRP mRNA were also observed in the diestrous rat (M. S. Smith, unpublished); the latter model was used for the rodent studies reported here. Immunohistochemical staining in the rat revealed a dense network of AGRP-positive fibers throughout the hypothalamus (Fig. 2, a and b). The specificity of the staining was confirmed by preabsorbing the hAGRP antibody with the peptide corresponding to the C-terminal residues 83–132 before the antibody was incubated with tissue sections (Fig. 2c). Dense AGRP fibers were found projecting from the arcuate to only

two divisions of the neuraxis, the hypothalamus and the septal region. In the hypothalamus, the densest fiber staining was observed originating in the arcuate and proceeding along the third ventricle as well as in the anterioperiventricular preoptic area, the periventricular nucleus, the parvocellular portion of the PVH, the dorsomedial nucleus (DMH), and the rostral end of the posterior nucleus (PH). Dense fiber staining was seen throughout the lateral and medial ARC. Scattered fiber staining was observed in the anterior and lateral hypothalamus (data not shown). Hypothalamic areas devoid of AGRP-positive fibers include the magnocellular portion of the PVH, the supraoptic nucleus, the suprachiasmatic nucleus (SCN), the ventromedial nucleus, and the compact zone of the DMH. The main extrahypothalamic projections led to the bed nucleus of the stria terminalis and the ventral part of the LS. Scattered fiber staining was also observed in the paraventricular nucleus of thalamus. No fibers were detected in the corpus striatum or the rostral portion of the brain stem. The caudal portion of the rat brain stem was not examined. Table 1 summarizes the regions in the CNS of the diestrous rat containing AGRP immunoreactivity.

AGRP immunoreactivity in the primate hypothalamus

Hypothalamic sections from fed and fasted male rhesus monkeys provided materials for the analysis of AGRP immunoreactivity. AGRP immunoreactivity was undetectable in the hypothalamus of the fed rhesus monkey (data not shown), but was readily visible in the fasted animal. As in the rat, dense hypothalamic fiber bundles were detected in the infundibular nucleus and projecting from there along the third ventricle. Dense fibers were observed in the PVH (Fig. 3a) and more caudally in the DMH (Fig. 3b). Also, as in the rat, a dense caudal fiber bundle was found in the septal region, predominantly in the stria terminalis (Fig. 4a) and LS region (Fig. 4b), passing through the medial preoptic area (Fig. 4c). In the rhesus, very dense fiber staining could be seen in the infundibulum (equivalent to the rodent median eminence, Fig. 4d), and cell bodies could be detected in the

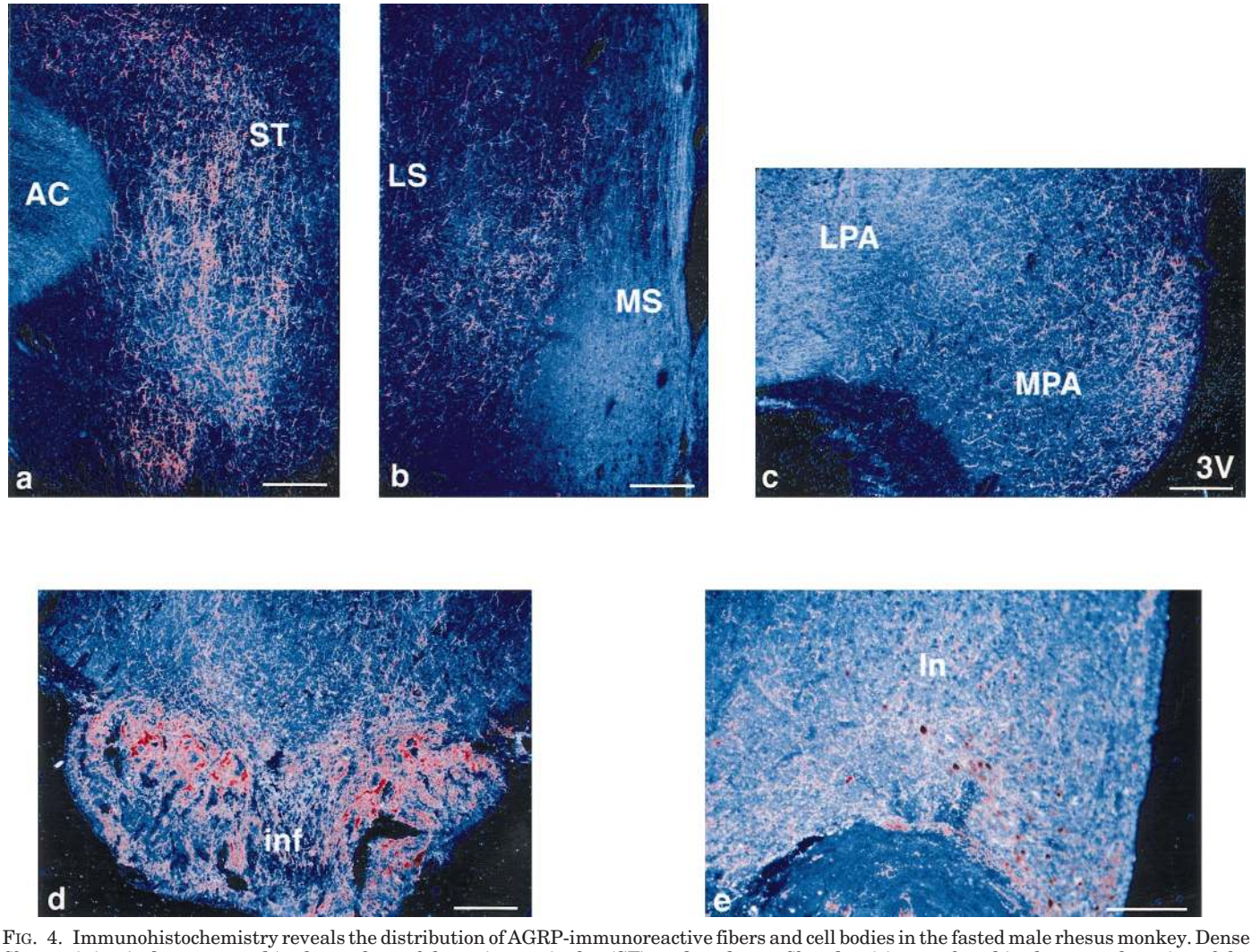

FIG. 4. Immunohistochemistry reveals the distribution of AGRP-immunoreactive fibers and cell bodies in the fasted male rhesus monkey. Dense fiber staining is demonstrated in the nucleus of the stria terminalus (ST), and moderate fiber densities are found in the ventral portion of the LS and the medial preoptic area (MPA). Very dense fiber staining is seen in the infundibulum (inf; d), and immunoreactive cell bodies are detectable in the infundibular nucleus (In; e). *Bars*, 50 μm (a–d) and 25 μm (e).

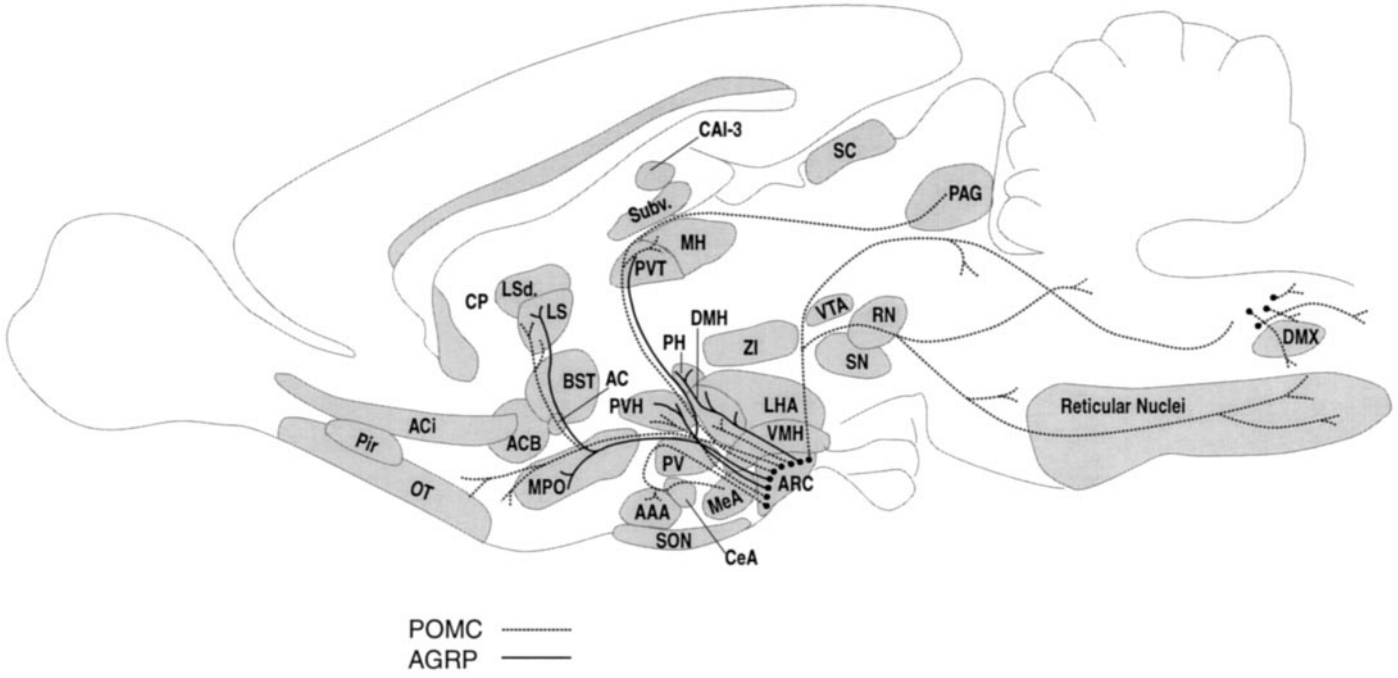

FIG. 5. Schematic diagram of a sagittal view of the rat brain, illustrating the comparative distributions of POMC and AGRP neurons. AAA, Anterior amygdaloid area; AC, anterior commissure; ACB, nucleus accumbens; Aci, anterior commissure; intrabulbar, ARH; arcuate nucleus of the hypothalamus; BST, bed nucleus of the stria terminalus; CA1–3, field CA1–CA3 of the hippocampus; CeA, central nucleus of the amygdala; CP, caudate putamen; DMX, dorsal motor nucleus of the vagus; LHA, lateral hypothalamic area; LSd, lateral septal area, dorsal aspect; MeA, medial amygdala; MH, medial habenula; MPO, medial preoptic area; OT, olfactory tubercle; PAG, periaquaductal gray; PH, posterior hypothalamus; Pir, piriform cortex; PV, periventricular zone; PVT, paraventricular nucleus of the thalamus; RN, red nucleus; SC, superior colliculus; SN, substantia nigra; SON, supraoptic nucleus; Subv, subiculum, ventral; VTA, ventral tegmental area; ZI, zona incerta. The locations of AGRP-immunoreactive fibers and cell bodies are based on data from the rat; fiber termini remain hypothetical. AGRP fiber distribution in the caudal brainstem was not examined in this study.

infundibular nucleus (Fig. 4e). Table 2 summarizes the AGRP-immunoreactive fibers distributed throughout the hypothalamus of the fasted male rhesus monkey. AGRP antiserum preabsorbed with control peptide, corresponding to the amino acids 83–132 mapping to the C-terminus of hAGRP, abolished all immunoreactivity (data not shown).

Discussion

AGRP-immunoreactive fibers in rat and rhesus monkey appear primarily in a subset of the same hypothalamic and septal brain regions containing dense POMC innervation (2, 31–33), with the densest fibers found innervating the PVH, DMH, posterior hypothalamus, and septal regions around the anterior commissure (Fig. 5). Within the rat hypothalamus, POMC fibers have a much wider distribution than AGRP, with moderate fiber density seen in just about every nucleus, with the possible exceptions of the VMH and supraoptic nucleus. A notable lack of AGRP fibers was observed in the VMH. These initial studies will, of course, need to be tempered by studies using additional antibodies, as it is possible that smaller amounts of immunoreactivity may be below the sensitivity of detection here, that the carboxyl-terminal epitope is specifically blocked in some brain regions, or that the immunoreactive epitope is unrecognizable in some brain regions as a consequence of proteolytic processing. Additionally, although the distributions reported here in the diestrous rat and fasted male rhesus are highly conserved, it will be important to determine whether the same distribution of immunoreactivity in the diestrous rat is seen in the fasted rat.

AGRP-immunoreactive fibers were also notably absent in the rat from additional divisions of the neuraxis receiving POMC fibers such as the rostral portion of the brain stem, hippocampus, amygdala, corpus striatum, and olfactory cortex tract (1–5). Remarkable conservation was seen in the distribution of AGRP fibers in rat and monkey; however, one striking difference was noted. Although AGRP fiber staining in the rat median eminence was limited and restricted to the lateral regions, very heavy fiber staining was seen in the rhesus infundibulum, suggesting the potential secretion of AGRP into the hypophyseal-portal circulation. Alternatively, this peptide could be acting at MSHα-binding sites in the infundibulum proper, as high levels of [^{125}I]NDP-α-MSH binding are observed in the rat median eminence (6) and thus may exist in the primate as well.

The overall distribution of AGRP-immunoreactive fibers represents a subset of regions that contain POMC projections and express MC3-R and MC4-R receptor mRNA hybridization (8, 9). These data thus further support the general hypothesis that AGRP serves as a locally delivered functional antagonist of the MC3-R and MC4-R (8, 9, 34). Although MC4-R is very widely distributed in the brain and has been demonstrated to be involved in feeding behavior and metabolism (18, 19), control of somatic growth (19), grooming

TABLE 2. Distribution of AGRP immunoreactivity in the rhesus central nervous system

Abbreviation	Anatomical brain region	Density
AA	Anterior hypothalamic area	+
Ac	Anterocentral n.	+
AH	Anterior hypothalamic n.	+
DA	Dorsal hypothalamic area	++
DBh	N. of diagonal band of Broca, horizontal portion	+
DBv	N. of diagonal band of Broca, vertical portion	++
DIn	Dorsal infundibular n.	++
DM	Dorsomedial n.	+
In	Infundibular n.	+++
Inf	Infundibulum	+++
itp	Inferior thalamic peduncle	+
La	Lateroanterior n.	+
LA	Lateral hypothalamic area	++
LS,v	Lateral septal n., ventral portion	++
LPA	Lateral preoptic area	+
Mes	Mesencephalictegmentum	+
MP	Medial preoptic n.	++
MPA	Medial preoptic area	+
MTM	Magnocellular tuberomammillary n.	+
PA	Posterior hypothalamic area	++
Pam	Paraventricular n., magnocellular group of anterior portion	+
Pap	Paraventricular n., parvocellular group of anterior portion	++
Pd	Paraventricular n., dorsal portion	+
Pea	Periventriculat n., anterior portion	++
Pem	Perimammillary n.	+
Pep	Periventricular n., preventricular portion	++
Pet	Periventricular n., tuberal portion	++
Pf	Perifornical n.	+
Pm	Paramammillary n.	+
Po	Posterior n.	+
pvn	Paraventricular n.	+
Sh	Septohypothalamic n.	+
SI	Substantia innominata	++
Soa	Supraoptic n.	+
Sot	Supraoptic n., tuberal portion	+
ST	N. of stria terminalis	+++
Sv	Subventricular n.	++
T	Tuberal n.	+
Vm	Ventromedial n.	+
VP	Ventral premammillary n.	+

Semiquantitative estimates of the signals are indicated based upon the number of fibers observed within a given area: + (weak); ++ (moderate); +++ (strong). Nomenclature is defined using a Rhesus monkey atlas (38).

behavior (23), control of the hypothalamic-pituitary-adrenal axis (23), febrile responses (24), and cardiovascular homeostasis (25), the data shown here suggest that AGRP may serve as a counterregulatory force in a more limited subset of these functions. In particular, the dense expression of AGRP in the PVH and DMH strongly imply a role for the peptide in energy homeostasis, as further supported by the observation that AGRP mRNA levels are regulated by leptin. In fact, preliminary data suggest that the melanocortin antagonist AGRP is much more robustly regulated by metabolic state than is the source of melanocortin agonist, POMC. For example, AGRP mRNA is up-regulated 5- to 10-fold in the *ob/ob* mouse (12, 13) compared with the 40–60% down-regulation reported for POMC mRNA in this model (35, 36). It is thus tempting to speculate that the main site for hormonal input to the melanocortin system in regard to regulation of energy homeostasis is at the AGRP neuron rather than the POMC neuron. A comparable example is seen in the pigmentary system, in which variable levels of agouti gene expression in the hair follicle act to modulate the effects of constitutive α-MSH on eumelanin synthesis in the melanocyte.

Acknowledgment

The authors thank Linda Cordilia for her work on the illustrations.

Note Added in Proof

While this manuscript was in proof, a detailed analysis of AGRP distribution in the mouse was reported (39).

References

1. **Watson SJ, Akil H, Richard CW, Barchas JD** 1978 Evidence for two separate opiate peptide neuronal systems and the coexistence of β-lipotropin, β-endorphin, and ACTH immunoreactivities in the same hypothalamic neurons. Nature 275:226–228
2. **Jacobowitz DM, O'Donohue TL** 1978 α-Melanocyte stimulating hormone: immunohistochemical identification and mapping in neurons of rat brain. Proc Natl Acad Sci USA 75:6300–6304
3. **Nilaver G, Zimmerman EA, Defendi R, Liotta A, Krieger DT, Brownstein MJ** 1979 Adrenocorticotropin and beta-lipotropin in the hypothalamus. Localization in the same arcuate neurons by sequential immunocytochemical procedures. J Cell Biol 81:50–58

4. **Joseph SA, Pilcher WH, Bennet-Clarke C** 1983 Immunocytochemical localization of ACTH parikarya in nucleus tractus solitarius: evidence for a second opiocortin neuronal system. Neurosci Lett 38:221–225
5. **Palkovits M, Mezey E, Eskay RL** 1987 Pro-opiomelanocortin-derived peptides (ACTH/β-endorphin/α-MSH) in brainstem baroreceptor areas of the rat. Brain Res 436:323–328
6. **Tatro JB** 1990 Melanotropin receptors in the brain are differentially distributed and recognize both corticotropin and α-melanocyte stimulating hormone. Brain Res 536:124–132
7. **Tatro JB, Entwistle ML** 1994 Distribution of melanocortin receptors in the lower brainstem of the rat. Ann NY Acad Sci 739:311–314
8. **Mountjoy KG, Mortrud MT, Low MJ, Simerly RB, Cone RD** 1994 Localization of the melanocortin-4 receptor (MC4-R) in neuroendocrine and autonomic control cirsuits in the brain. Mol Endocrinol 8:1298–1308
9. **Roselli-Rehfuss L, Mountjoy KG, Robbins LS, Mortrud MT, Low MJ, Tatro JB, Entwistle ML, Simerly R, Cone RD** 1993 Identification of a receptor for γ-MSH and other proopiomelanocortin peptides in the hypothalamus and limbic system. Proc Natl Acad Sci USA 90:8856–8860
10. **Gantz I, Konda Y, Tashiro T, Shimoto Y, Miwa H, Munzert G, Watson SJ, DelValle J, Yamada T** 1993 Molecular cloning of a novel melanocortin receptor. J Biol Chem 268:8246–8250
11. **Gantz I, Miwa H, Konda Y, Shimoto Y, Tashiro T, Watson SJ, DelValle J, Yamada T** 1993 Molecular cloning, expression, and gene localization of a fourth melanocortin receptor. J Biol Chem 268:15174–15179
12. **Shutter JR, Graham M, Kinsey AC, Scully S, Luthy R, Stark KL** 1997 Hypothalamic expression of ART, a novel gene related to agouti, is upregulated in *obese* and *diabetic* mutant mice. Genes Dev 11:593–602
13. **Ollmann MM, Wilson BD, Yang Y-K, Kerns JA, Chen Y, Gantz I, Barsh GS** 1997 Antagonism of central melanocortin receptors in vitro and in vivo by agouti-related protein. Science 278:135–137
14. **Lu D, Willard D, Patel IR, Kadwell S, Overton L, Kost T, Luther M, Chen W, Woychik RP, Wilkison WO, Cone RD** 1994 Agouti protein is an antagonist of the melanocyte-stimulating hormone receptor. Nature 371:799–802
15. **Miller MW, Duhl DMJ, Vrieling H, Cordes SP, Ollmann MM, Winkes BM, Barsh GS** 1993 Cloning of the mouse *agouti* gene predicts a novel secreted protein ubiquitously expressed in mice carrying the *lethal yellow* (*Ay*) mutation. Genes Dev 7:454–467
16. **Bultman SJ, Klebig ML, Michaud EJ, Sweet HO, Davisson MT, Woychik RP** 1994 Molecular analysis of reverse mutations from nonagouti (*a*) to black-and-tan (*at*) and white-bellied agouti (*Aw*) reveals alternative forms of agouti transcripts. Genes Dev 8:481–490
17. **Yen TT, Gill AM, Frigeri LG, Barsh GS, Wolff GL** 1994 Obesity, diabetes, and neoplasia in yellow *Avy*/− mice: ectopic expression of the *agouti* gene. FASEB J 8:479–488
18. **Fan W, Boston BA, Kesterson RA, Hruby VJ, Cone RD** 1997 Role of melanocortinergic neurons in feeding and the agouti obesity syndrome. Nature 385:165–168
19. **Huszar D, Lynch CA, Fairchild-Huntress V, Dunmore JH, Fang Q, Berkemeier LR, Gu W, Kesterson RA, Boston BA, Cone RD, Smith FJ, Campfield LA, Burn P, Lee F** 1997 Targeted disruption of the melanocortin-4 receptor results in obesity in mice. Cell 88:131–141
20. **Fong TM, Mao C, MacNeil C, Kalyani R, Smith T, Weinberg D, Tota MR, Van der Ploeg LH** 1997 ART (protein product of agouti-related transcript) as an antagonist of MC-3 and MC-4 receptors. Biochem Biophys Res Commun 237:629–631
21. **Graham M, Shutter JR, Sarmiento U, Sarosi I, Stark KL** 1997 Overexpression of Agrt leads to obesity in transgenic mice. Nat Genet 17:273–274
22. **Wolff GL** 1990 Obesity, cancer, and the viable yellow *Avy/a* mouse. Discrimination among pathophysiological effects of the expression of the *Avy/a* genotype in obese and lean mice. In: Oomura Y (eds) Progress in Obesity Research, chapt 70. Libbey, pp 445–448
23. **Von Frijtag JC, Croiset G, Gispen WH, Adan RA, Wiegant VM** 1998 The role of central melanocortin receptors in the activation of the hypothalamus-pituitary-adrenal-axis and the induction of excessive grooming. Br J Pharmacol 123:1503–1508
24. **Huang Q-H, Entwistle ML, Alvaro JD, Duman RS, Hruby VJ, Tatro JB** 1997 Antipyretic role of endogenous melanocortins mediated by central melanocortin receptors during endotoxin-induced fever. J Neurosci 17:3343–3351
25. **Li S-J, Varga K, Archer P, Hruby VJ, Sharma SD, Kesterson RA, Cone RD, Kunos G** 1996 Melanocortin antagonists define two distinct pathways of cardiovascular control by α- and γ-melanocyte-stimulating hormones. J Neurosci 16:5182–5188
26. **Schreihofer DA, Amico JA, Cameron JL** 1993 Reversal of fasting-induced suppression of luteinizing hormone (LH) secretion in male rhesus monkey by intragastric nutrient infusion: evidence of rapid stimulation of LH by nutritional signals. Endocrinology 132:1890–1897
27. **Cameron JL, Nosbisch C** 1991 Slowing of pulsatile LH and testosterone secretion during short-term fasting in adult male rhesus monkeys (*Macaca mulatta*). Endocrinology 128:1532–1540
28. **Johansson O, Backman J** 1983 Enhancement of immunoperoxidase staining using osmium tetroxide. J Neurosci Methods 7:185–193
29. **Arriza JL, Stoler MH, Angerer RC** 1988 The neuronal mineralocorticoid receptor as a mediator of glucocorticoid response. Neuron 1:887–900
30. **Quillan JM, Sadee W, Wei ET, Jimenez C, Ji L, Chang JK** 1998 A synthetic human agouti-related protein-(83–132)-NH2 fragment is a potent inhibitor of melanocortin receptor function. FEBS Lett 428:59–62
31. **Finley JCW, Lindstrom P, Petrusz P** 1981 Immunocytochemical localization of β-endorphin-containing neurons in the rat brain. Neuroendocrinology 33:28–42
32. **Khachaturian H, Lewis ME, Haber SN, Akil H, Watson SJ** 1984 Proopiomelanocortin peptide immunocytochemistry in rhesus monkey brain. Brain Res Bull 13:785–800
33. **Watson SJ, Barchas JD, Li CH** 1977 β-Lipotropin: Localization of cells and axons in rat brain by immunocytochemistry. Proc Natl Acad Sci USA 74:5155–5158
34. **Low MJ, Simerly RD, Cone RD** 1994 Receptors for the melanocortin peptides in the central nervous system. Curr Opin Endocrinol Diabetes 1:79–88
35. **Mizuno TM, Kleopoulos SP, Bergen HT, Roberts JL, Priest CA, Mobbs CV** 1998 Hypothalamic pro-opiomelanocortin mRNA is reduced by fasting and corrected in *ob/ob* and *db/db* mice, but is stimulated by leptin. Diabetes 47:294–297
36. **Thornton JE, Cheung CC, Clifton DK, Steiner RA** 1997 Regulation of hypothalamic proopiomelanocortin mRNA by leptin in *ob/ob* mice. Endocrinology 138:5063–5066
37. **Paxinos G, Watson C** 1997 The Rat Brain in Stereotaxic Coordinates. Academic Press, San Diego
38. **Bleier R** 1984 The Hypothalamus of the Rhesus Monkey: A Cytoarchitectonic Atlas. University of Wisconsin Press, Madison
39. **Broberger C, Johansen J, Johansson C, Schalling M, Hokfelt T** 1998 The neuropeptide Y/agouti gene-related protein (AGRP) brain circuitry in normal, anorectic, and monosodium glutamate-treated mice. Proc Natl Acad Sci USA 95:15043–15048